ENERGY FLOW ANALYSIS ON A MULTI-ZONAL BUILDING SCALE USING SANKEY DIAGRAMS

Aly Abdelalim, Zixiao Shi, William O'Brien
Human-Building Interaction Lab Carleton University 1125 Colonel by Dr. Ottawa, ON K1S 5B6 Canada
{AlyAbdelalim, zixiaoshi}@cmail.carleton.ca, liam.obrien@carleton.ca

Keywords
Energy flows in buildings, calibration methods, BPS (building performance simulation), Sankey diagrams.

ABSTRACT
Modern commercial buildings have complex mechanical systems and heat transfer paths, and their performance is typically difficult to visualize. Current data availability and visualization tools do not lend themselves well to identifying inefficiencies and possible solutions. Sankey diagrams have been found to be useful tool in energy management and performance improvement. However, there are limited existing applications on the building level. This paper proposes a method to estimate and visualize energy flow on the building level. The objective is to demonstrate the applicability of Sankey diagrams to identify opportunities for energy savings. The proposed methodology is then applied to an 8,000 m^2 multi-zone Canadian university building. Data for resource consumption were obtained from meters and sensors installed in the building. While building energy performance data were obtained from a calibrated building performance simulation (BPS) model of the building to understand the interrelated variables that affect building performance. The outcome of this work is to help identify and quantify the significant measured and unmeasured energy flows.

INTRODUCTION
Nowadays, commercial and institutional buildings sector energy demand is significantly increasing (NRCan, 2014). Most of modern buildings utilize energy management and control systems (EMCS) for monitoring and optimizing building systems during operation. EMCS could provide spatial and temporal data resolution obtained from meters and sensors installed in buildings. However, the data from metering and logging systems are often inconvenient and difficult to access due to use of multiple systems and technologies of varying vintages and platforms.

Furthermore, most of the developed visualization tools for building energy management use simple line or bar charts for presenting and comparing metered energy consumption, greenhouse gasses (GHG) emissions, and other performance metrics (Yarbrough et al., 2014). On the building level, Pulse Energy developed an Energy Dashboard tool that shows real-time building consumption of energy, natural gas, hot water, chilled water, and steam for campus buildings (UBC, 2014 a; McGill University, 2015). Other tools such as Building Dashboard and Energy Efficient Education Dashboard were developed to visualize energy consumption of commercial buildings (Lucid, 2014). The current visualization tools typically only provide an end-use breakdown of energy consumption, depending on installed meter resolution. However, these tools are difficult to provide a comprehensive energy flow analysis on the building scale (i.e. how energy enters and is consumed in buildings). Furthermore, the current data availability and visualization tools do not lend themselves to identification of inefficiencies and possible solutions to improve efficiency or recover energy.

Many researchers have been focusing on analyzing and visualizing building energy use (Belzer, 2006; Abdelalim et al., 2015). The building gross energy needs should be quantified, which represents the anticipated buildings energy demands for heating, cooling, lighting, refrigeration, water heating, and equipment. The building's energy demand is determined by different parameters, such as indoor climate requirements, outdoor climatic conditions, building envelope thermal properties, and infiltration rates (Santamouris, 2010). There are also opportunities for recovering energy and understanding the relationship between heat gains and heating and cooling loads. For instance, the choice of light bulbs/fixtures should incorporate their impact on heating and cooling loads. On the other hand, Sankey diagrams can provide relative flow magnitudes, direction of flows, inputs and outputs of interacting systems, and energy recovery. Moreover, spatial representation (e.g., the order of systems and components can be approximately laid out in a Sankey diagram).

A study by (Abdelalim et al., 2015) proposed several methods to analyze and visualize building-level water, natural gas, and electricity consumption and the upstream environmental impacts using Sankey diagrams and other graphical techniques. Belzer (Belzer, 2006) developed energy flow maps to depict

energy flows from source to end-use in the building sector using Sankey diagrams. The end-use consumption was based on estimations from Building Energy Data-book (BED). Another application used dynamic Sankey diagrams to visualize internal and external flows through the envelope (phineas, 2015). The study helped in visualizing the amount of energy hitting and leaving the façade by radiation and convection. The study only included the required heating and cooling to maintain an acceptable indoor air temperature. A study by (O'Brien, 2012) addressed major issues involved in creating Sankey diagrams to represent building energy flows of a solar house obtained from a BPS model. A limited number of building design and analysis tools, such as CASAnova software (Heidt, 2012) and Sefaira (Sefaira, 2012) use Sankey diagrams for visualizing predicted energy use.

This paper proposes a method to analyze and visualize energy flow by using historical data obtained from EMCS and a calibrated BPS model to form a comprehensive energy use assessment at the building level. The objective of this paper is to make operational problems more visible and quantifiable in order to identify opportunities for energy savings and to facilitate the decision-making by building operators, campus planners, and other stakeholders. Moreover, it will help in estimating and understanding the impact of unmeasured energy flows (for instance, solar gains, heat loss from infiltration, etc.). The proposed method is then applied to a case study: the Canal Building at Carleton University in Ottawa, Canada. The main objective of this research is to develop a method to obtain, process, analyze, and visualize energy flow of a multi-zonal, mixed-use commercial building. Within the scope of this work, by using a combination of measured data and models, a comprehensive energy use assessment at the building-level can be formed.

METHODOLOGY

The main objective of this study is to combine measured and modelled data to provide a comprehensive energy use assessment as shown in Figure 1. EMCS provides real-time and historical energy consumption data, which are obtained from meters and sensors for some components such as lighting, equipment/appliances, elevators, AHUs (air handling units) components, VAV (variable air volume)-reheat coils, radiant panels, chillers, pumps, and steam. However, some other variables are impractical and difficult to meter such as internal gains, solar gains, infiltration rates, opaque envelope heat loss, and window heat loss. These variables could be approximated using a calibrated BPS (building performance simulation) model based on many modelling assumptions and simplifications. EnergyPlus 8.1 (E+) was selected as the BPS tool due to its technical documentation and versatility and capability of simulating complex building systems (Dong et al., 2014). Moreover, it is crucial to ensure that the BPS model is able to closely represent the actual behavior of the building under study. This can

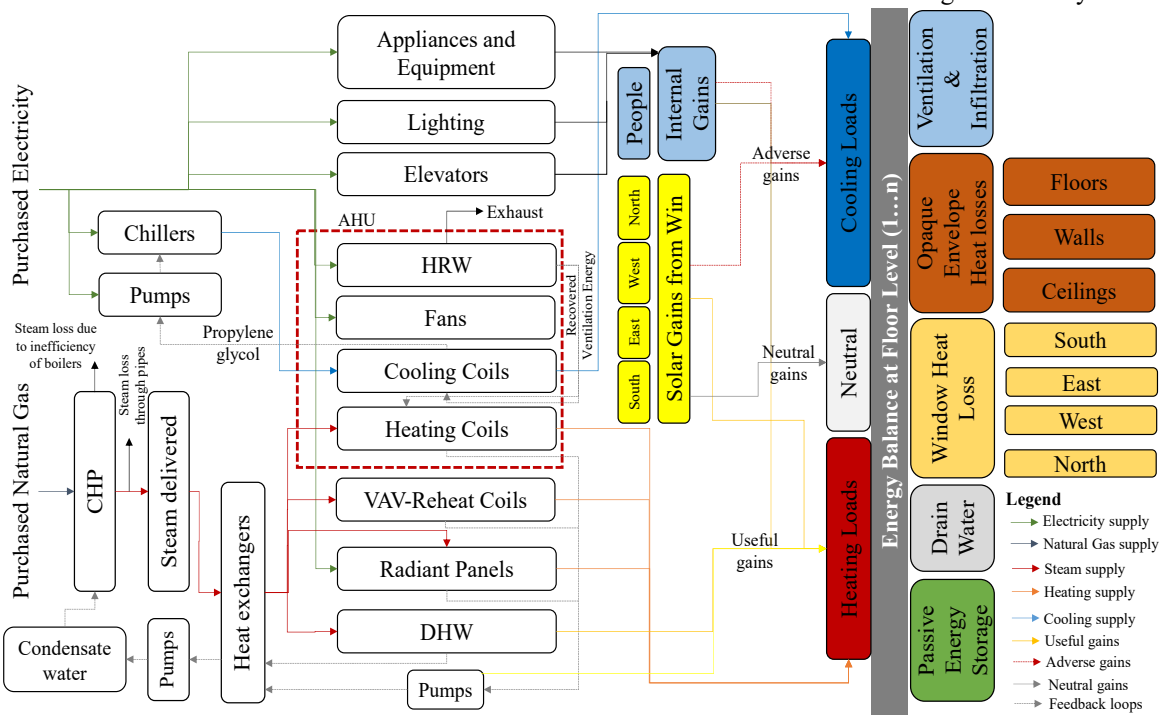

Figure 1: Flowchart showing the main scope of the study on the building level

be achieved by calibrating the model against the measured data.

At first, this paper discusses the supplied and delivered energy sources (i.e. supplied energy for heating and cooling loads), energy from solar irradiation, internal gains, and sources of heat losses through the building envelope. The methodology focuses on developing energy balances based on measured and modelled data for different components on the building level (i.e. HVAC system, appliances/ equipment, lighting, elevators, and building envelope). The following energy balance equations of each component are written in terms of final (secondary) energy, making use of the following symbols: thermal energy Q, including all incoming (positive) and outgoing/ extracted (negative) energy. While, $\dot{m}$ is the mass flow rate of fluids, C_p is the specific heat capacity, and T and h are the temperature and enthalpy of fluids, respectively. U is the overall heat transmission loss, and A is the effective area of exposed surface, T_{in} and T_{out} are the inside and outside air temperature, respectively. All units are in SI. These equations are steady state energy balances (i.e. they do not include thermal storage terms). This assumption is formed on the basis that net energy stored during longer periods is not significant compared to energy flows. However, dynamic heat transfer through the building envelope is resolved in the calibrated EnergyPlus model. The study focused on sub-hourly data for two weeks in winter and summer. Shorter periods would require a closer examination of internal heat storage.

The study then focusses on calibrating the BPS model in order to obtain sub-hourly data to create a comprehensive energy-use assessment using Sankey diagrams on the building-level.

SUPPLIED AND DELIVERED ENERGY

The supplied energy is also known as the secondary energy. The supplied energy is often metered to record the consumption of the building. The supplied energy is converted to another form by means of a conversion system installed in the building such as the conversion of natural gas to heat by using boilers. The output from the supplied conversion systems is thermal energy, which is known as the delivered energy (Santamouris, 2010). The delivered energy is divided into five utilization types: energy for space heating, energy for space cooling, energy for district water heating, energy for internal appliances/equipment, and energy for external appliances. On the other hand, energy from solar irradiance and energy from metabolism (i.e. from occupants) are not counted as delivered energy. In the scope of this work, the amount of energy required for domestic water heating is considered negligible compared to the amount of energy required for space heating because the case study building does not have kitchens or showers – only a limited number of low-flow washroom sinks. The following sections discuss the energy gains and losses for the above-mentioned utilization types.

Heating Loads

The amount of energy required for space heating is the amount of energy delivered from heating units to the heated spaces during heating season as shown in Eq. (1). In the context of the selected study, the building relies on the steam generated at the central heating plant (CHP). The steam delivered from the central heating plant (CHP) passes through a heat exchanger that uses the thermal energy to provide heat to the heating coils, variable-air-volume (VAV-reheat coils), and radiant panels.

$$Q_{Space\ heating} = Q_{Heating\ coils} + Q_{Radiant\ panels} + Q_{Solar} \; Q_{VAV\text{-}reheat\ coils} + Q_{Internal\ gains} - Q^{building\ envelope}_{gains/losses} \quad (1)$$

For the heating coils, energy is transferred from the hot water to the air stream running through the exchanger. The amount of thermal energy is expressed in Eq. (2).

$$Q_{Heating\ coils} = \dot{m}_{HW} \times C_P(T_{HW,\,avg}) \times (T_{HW,supply} - T_{HW,return}) = \dot{m}_{air} \times C_P(T_{air,\,avg}) \times (T_{air,leaving\ heating\ coil} - T_{air,entering\ heating\ coil}) \quad (2)$$

where, the subscript *HW* refers to hot glycol water. For the radiant ceiling panels installed in some spaces in the building, the energy balance is shown in Eq. (3).

$$Q_{radiant\ panel} = \dot{m}_{HW} \times C_P(T_{HW,\,avg}) \times (T_{HW,supply} - T_{HW,return}) \quad (3)$$

Some VAV-boxes installed in commercial buildings contain reheat coils. The amount of thermal energy from the VAV-reheat coils is shown in Eq. (4).

$$Q_{VAV\text{-}reheat\ coils} = \dot{m}_{HW} \times C_P(T_{HW,\,avg}) \times (T_{HW,supply} - T_{HW,return}) \quad (4)$$

Mass flow rates, and temperatures of air and hot water can often be obtained from EMCS. Moreover, operational schedules can be obtained from EMCS.

Cooling Loads

The amount of energy required for space cooling is shown in Eq. (5).

$$Q_{Space\ cooling} = Q_{Solar} + Q_{Internal\ gains} + Q^{building\ envelope}_{gains/losses} \quad (5)$$

The refrigerant (water-propylene glycol for the case study building) extracts energy from the water in the

evaporator and transfers it to condensing water by means of a vapour compression cycle. The amount of energy gained from the evaporator is expressed in Eq. (6).

$$Q_{Cooling\ coil} = \dot{m}_{CHW} \times (h_{in}-h_{out}) = \dot{m}_{CHW} \times C_p \times (T_{in}-T_{out}) \quad (6)$$

where, the subscript *CHW* is the chilled water. Energy gains from solar and internal gains and sources of heat losses or gains through the building envelope are discussed below.

Energy from Internal Gains

Internal gain sources that affects heating and cooling loads in commercial buildings are lighting, equipment, and occupants. The required energy for equipment and lighting is the sum of energy dissipated from the units within the building envelope. The energy balance for lighting and equipment is approximated as Eq. (7).

$$Q_{Lighting/equipment} = \sum P_{Lighting/equipment} \quad (7)$$

Where P is the amount of electrical energy consumption. This assumption is on the basis that all consumed electrical power is converted into thermal energy. Some are transferred by a percentage radiation, latent, and convection. On the other hand, the metabolic rate of occupants directly converts to sensible and latent energy. The dissipated energy is shown in Eq. (8).

$$Q_{Occupants} = \sum_{i=1}^{n} M_i \quad (8)$$

where M_i is the metabolic rate and n is the number of occupants. The metabolic rate is the sum of sensible and latent heat gains.

The amount of energy gained from solar radiation, lighting, and equipment can offset to the heating loads (i.e. useful gains). On the other hand, it could increase the cooling loads by which more purchased electrical energy is required (i.e. adverse gains). Furthermore, during shoulder seasons, these gains may not affect heating and cooling loads (i.e. neutral gains), if the indoor air temperature remains within the range of heating and cooling setpoint and does not trigger free cooling (O'Brien, 2012).

Sources of Energy Loss/Gains through the Building Envelope

The amount of solar radiation that is transmitted into the building through glazed surfaces requires information on geometry, orientation, shading, and topography (Santamouris, 2010). The rate of net energy gain through glazing is expressed in Eq. (9).

$$Q_{Solar} = \sum A_j \times [SHGC(\Theta) \times I_{solar} - U \times (T_{in} - T_{out})] \quad (9)$$

where *SHGC* is the solar heat gain coefficient, which is a function of angle of incidence of solar radiation. While, I_{solar} is the amount of solar radiations and diffuse irradiance hitting the surface A in the orientation j.

Sources of energy gain or loss through the building envelope are from conduction through the envelope, shortwave and longwave radiation exchange, natural ventilation, and infiltration heat transfer. Another source of heat loss is from the conduction through the foundation or basement.

Equation (10) shows transient one-dimensional heat conduction through a homogeneous layer with constant thermal properties, neglecting storage terms.

$$Q^{Conduction}_{gains/losses} = -k \times A \times \frac{\Delta T}{\Delta x} \quad (10)$$

Where, k is the thermal conductivity and the temperature is a function of position x. In case of conduction through the foundation or basement, T_o (outdoor air temperature) be replaced by T_e, which is the ground temperature. The ground temperature is a function of incident solar radiation, rainfall, seasonal swings of air temperature, local vegetation cover, type of soil, and depth in the earth.

Infiltration rates affect heating and cooling loads. Sources of infiltration are from leakage in the building construction and opening and closing of windows and exterior doors. The value is difficult to predict by using BAS (Building Automation System)-related sensors and meters as it depends on several variables, such as wind speed, difference between outside and inside temperatures, the quality of the building construction, etc. (Gowri et al., 2009; Ng et al., 2015). Energy losses or gains from infiltration is calculated as shown in Eq. (11).

$$Q^{infiltration}_{gains/losses} = \sum [\rho \times Q \times V \times (h_{in} - h_{out})] \quad (11)$$

Where, ρ is the density of air, Q is the number of air changes per unit time, h is the enthalpy, and V is the room volume.

Ventilation rates also affect heating and cooling loads. The energy losses or gains by ventilation taking into account the heat recovery wheel (HRW) is shown in Eq. (12).

$$Q^{ventilation}_{gains/losses} = \sum [(1 - \eta) \times \rho \times q_v \times (h_{in} - h_{out})] \quad (12)$$

Where, η is the efficiency of the heat recovery wheel and q_v is the volumetric airflow rate.

MODEL CALIBRATION

This study proposes a hybrid calibration method: an evidence-based method by (Raftery et al., 2011) and an analytical optimization method by Sun et al. (Sun & Reddy, 2006). Evidence-based methods use a manual input calibration procedure that relies on evidence obtained from design drawings, measurements, sensor readings, etc. Although, this method provides a hierarchy of evidence reliability and version control, it can be time consuming and adequate evidence is not always available for all inputs.

On the other hand, the analytical optimization method uses a mathematical and statistical procedure to automatically optimize the input values so that measurements match simulation predictions. However, adjusting a high number of unknown parameters can still yield unsatisfactory results, so some form of input parameters calibration before analytical optimization is required (Sun & Reddy, 2006). In order to overcome the limitations of both methods, (Coakley et al., 2012) developed a joined evidence-based and analytical optimization method and was adopted in this study. Figure 2 shows the proposed calibration methods.

The evidence-based calibration method is applicable for most parameters in the building model since the case study selected (Canal Building at Carleton) has a large and growing pool of evidence. Significant effort has been dedicated to this ongoing calibration process. In some cases, an on-site audit was required to determine the number and types of equipment used in each zone as this information is not documented and there is no sub-metering in individual rooms and labs.

In the context of the selected case study, the data obtained from EMCS include only consolidated electricity data for each floor. However, BPS tools such as EnergyPlus require hourly schedules for each zone. In this study, an inverse calibration procedure was developed to tune lighting, equipment power densities and schedules based on the proposed method by (Lam, et al., 2014). A Matlab script was written to automate the process of obtaining hourly schedules for each zone as shown in Figure 3. The method follows six steps: 1) assumed power density based on on-site audit for each room in the building; 2) constraints are set for operational hours based on on-site observations; 3) hourly computed power for lighting and equipment are compared to actual measured data to meet the MBE and CV(RMSE) criterion for each floor; 4) if the criteria are not met, based on the room type (hallways, offices, classrooms, teaching labs, café, or mechanical rooms), an hourly inverse calibration factor, calculated by taking the hourly measured power (P), divided by the computed power (P-simulated) taking into account operational hours, will be multiplied by the hourly schedule; 5) the calibrated power densities are calculated by

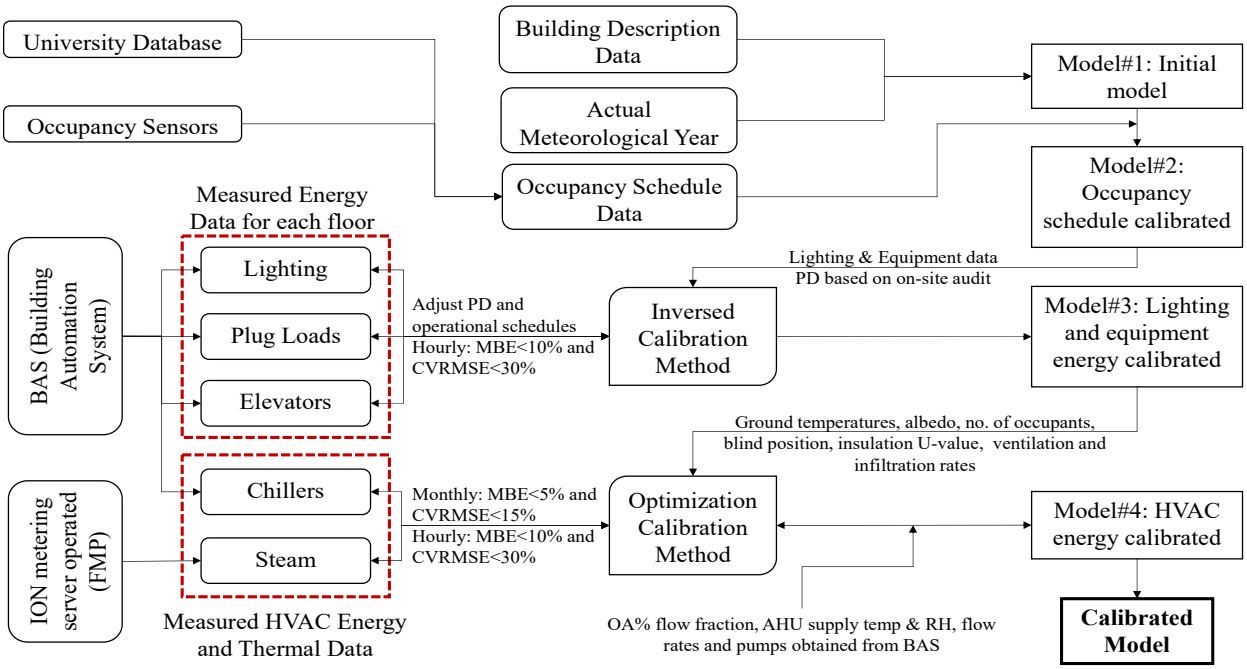

Figure 2: Proposed building energy model calibration methods

multiplying the calibration factor by the assumed lighting and equipment densities; and, 6) if the criteria are met, an 8760-hour schedule including weekdays, weekends, and national holidays is generated to input in EnergyPlus.

Some model parameters are difficult to obtain and have significant impact on the building performance, such as thickness and thermo-physical properties of materials, blind positions, ground temperatures, albedo, number of occupants (user behavior uncertainties), and ventilation and infiltration rates (Silva & Ghisi, 2014). Thus, the optimization method is applied as it helps in identifying a set of input parameter values that minimize an objective function during the calculation of simulation cases. The objective function as recommended by ASHRAE 14-2002 is to achieve Mean Bias Error (MBE) of ± 10% and Coefficient of Variation of the Root Mean Square Error CV(RMSE) of ± 30% when calibrating hourly data.

ExCalibBEM tool developed by Hydro Quebec was used in order to facilitate building model calibration to measured data (Simeb, 2011; LBNL, 2011). This tool is a graphical interface for GenOpt. The optimization algorithm used in this research is Generalized Pattern Search algorithm (GPSHookeJeeves) which is useful to obtain optimal solution versus the number of evaluation when dealing with continuous parameters.

The ventilation opening area refers to a fraction representing the effective area of the total operable window area available for natural ventilation ranging from 0 to 1 (Silva & Ghisi, 2014).

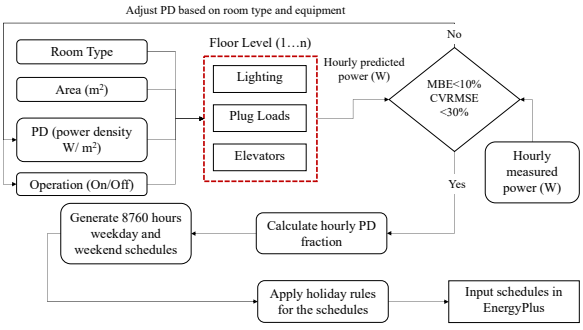

Figure 3: The inverse calibration procedure

For the airflow coefficient through opening cracks, the work by Liddament (Liddament, 1986) was considered, defining values for lower, mode and upper, which will be used in a triangular probability distribution. The albedo (reflectance of the ground surface) was adopted as a triangular distribution with values ranging from 0.13 to 0.26 for climates without snow and 0.5 to 0.7 in the presence of snow according to Thevenard and Haddad (Thevenard & Haddad, 2006). For ground temperature, an uncertainty of ±4°C (Silva & Ghisi, 2014) of standard deviation for each month of the year was considered, based on the CWEC (Canadian Weather for Energy Calculations) weather file. For the insulation thermal resistance, the work of (MacDonald, 2002) was taken as a basis, which considers the sum of the systematic uncertainties (differences in temperature, humidity and age of the material). The number of occupants in each classroom will be represented by a fraction ranging from 0 to 1 with an increment of 0.1 of the total capacity of each classroom (Silva & Ghisi, 2014). The blind position refers to a fraction representing the effective area available for blocking direct solar radiations ranging from 0 to 1.

MODELLING APPROACH IN ENERGYPLUS (E+)

One of the crucial steps that has to be considered is the modeling approach used in energy simulation tools (EnergyPlus in this case) as stated by (Heo, 2011). EnergyPlus uses "Heat balance" method in determining zone thermal response, by which room air is modeled as well mixed with uniform temperature throughout each zone. The heat balance model is also applied to external and internal surfaces, where room surfaces have uniform surface temperatures, uniform long and short wave irradiation, diffuse radiating surfaces, and internal heat conduction. The Surface Heat Balance Module simulates an inside and outside surface heat balance, interconnections between heat balances and boundary conditions, conduction, convection, radiation, and mass transfer (water vapor) effects. The Air Mass Balance Module deals with various mass streams such as ventilation and exhaust air, and infiltration rates. It accounts for thermal mass of zone air and evaluates direct convective heat gains. Thus, the following discussion covers the modeling approaches chosen for the current case study.

For conductive heat transfer, CTFs (conduction transfer functions) for transient conduction through the opaque envelope was selected, as the material's thermo-physical properties were assumed to not vary with temperature. For the inside convection algorithm, as not all zones have the same configurations for diffusers, thus it is recommended by (US-DOE, 2009) to use adaptive convection algorithm developed by (Beausoleil-Morrison, 2002). This method provides a dynamic selection of convection models based on conditions. The same algorithm was selected for the outside convection algorithm.

For diffuse sky radiation, EnergyPlus uses anisotropic sky model by (Perez et al., 1990). As well as,

EnergyPlus has the ability to define different monthly values for albedo. For window properties, Window LBNL was used to obtain values for SHGC, U-value, solar and visible transmittance, and spectral data. For the transmitted beam radiation, the default model was selected, as some zones in the model are non-convex zones. The assumption in the default model is that all transmitted beam radiation strikes the floor, some is absorbed based on the absorptivity of materials, and some is reflected based on an area weighting. Moreover, shading (aka shadowing) is calculated by default every 20 days. Only shading of sky diffuse is treated, while shading of ground-reflected diffuse is not considered in simulations. For view factors between internal surfaces, EnergyPlus calculations are determined by area weighted and also limited to "seen" surfaces.

For the infiltration model, ACH (air changes hour) method is selected to calculate infiltration rates. Infiltration is specified as a design level, which is modified, by a schedule fraction based on temperature difference and wind speed. Thus, it is not constant over the whole year. Moreover, the calculated option increases the complexity of the model and slows simulations down. Since an optimization of different parameters will be followed, the scheduled option was selected (US-DOE, 2009).

US-DOE recommended time steps of ten minutes in the case of building simulation models that include HVAC (US-DOE, 2009). A detailed HVAC system was modelled in DesignBuilder (a graphical interface for EnergyPlus). The detailed HVAC model enables definition of air loops, plant and condenser loops, HVAC zone groups, system control and set point managers, and sizing of HVAC flow rates. Both the heating water and chilled water distribution loops in the building are modeled as variable flow systems. A sequential distribution scheme was also selected as it operates equipment in a serial manner based on the loop operation scheme (which assigns priority to different equipment on the loop). When highest priority equipment is out of capacity, the next highest priority equipment tries to meet the load, etc. For modelling the hot water plant loop, it is required to model boiler and specify its efficiency. In the context of Canal Building, steam delivered to the building is produced by the CHP. Thus, two modelling options are available: either by using district heating or using a high boiler efficiency (100 percent). The district heating is only available in simple HVAC models, thus a boiler with high efficiency was selected.

CASE STUDY

The Canal Building was selected for the case study as it includes a large variety of functional space such as private offices, open-plan offices, lecture rooms, computer labs, design labs, research labs, conference rooms and other facility rooms. The building is also equipped with more than 2500 sensors to collect data required to inspect hourly energy consumption for each floor. The building began operating in 2011. Building details are summarized as follows:

General	Area (m^2)	8,000
	No. of stories (including basement)	7
	No. of modelled zones	174
	Bldg. type	Mixed-use academic
Building Envelope U-value ($W/m^2.K$)	Roof	0.3
	Walls	0.47 to 0.24
	Foundation walls	0.53
	Intermediate floor	2.5
	Windows (double-glazed with air gaps of 13.5mm)	2.67
	Window (SHGC)	0.722
HVAC air loop	Two small air-handling units (AHU) are designated for the mechanical rooms, while, the rest of the building is conditioned by two separate identical AHU units. Single duct VAV-box; non-corner spaces' VAV boxes contain reheat coils	
Chiller	ElectricEIRChiller Centrifugal Carrier 19XR 1407kW/6.04COP/VSD	
Space heating	Relies on the steam generated at a central plant. Some perimeter rooms are equipped with radiant panels	
Thermostat settings	heating /cooling setpoints are variable (ranges from 20°C to 24°C)	

A higher model resolution was required as the study focused on the performance of the spaces per each floor. Moreover, some of the rooms share the same VAV-box or the air is supplied by two or more VAV-boxes. Furthermore, rooms have different occupancy patterns, by which these zones cannot be merged. Figure 4 shows the BPS model for the Canal Building. Figure 5 shows different zone activities and boundary conditions for the fourth floor (as an example) of Canal Building. Furthermore, AMY (actual meteorological year) was used for Ottawa, Canada to obtain weather data based on the NOAA/NCEP Climate Forecast System Reanalysis (CFSR) model (U.S. Department of Energy, 2014).

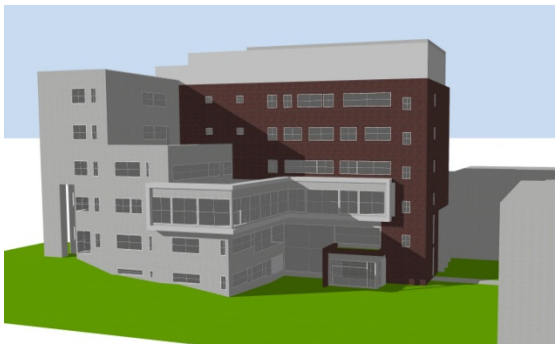

Figure 4: Canal Building BPS model

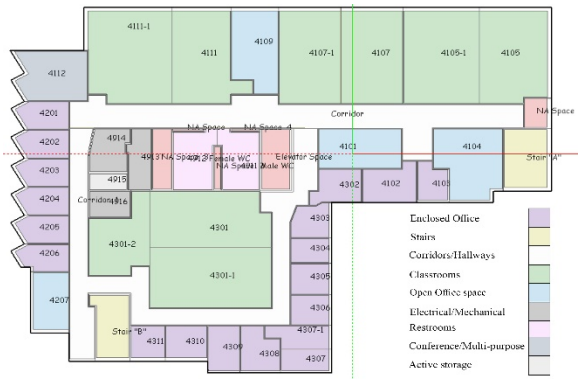

Figure 5: Canal Building fourth floor showing different zone activities

RESULTS AND DISCUSSION

The aim of this study is to analyze and visualize energy flow on the building-level using data from meters and BPS model. The study focuses on two weeks in winter (1st to 15th of February) and summer (1st to 15th of July). Preliminary calibration results showed that lighting energy and plug loads have good agreement with the measured data. Hourly MBE (mean bias error) and CV (RMSE) (coefficient of variation of root mean square error) for lighting energy are -0.03% and 0.07%, respectively. While, for plug loads, hourly MBE and CV (RMSE) are 0.02% and 0.05%, respectively. On the other hand, the heating and cooling loads showed less agreement with measured data as shown in Figure 6 and Figure 7, respectively. This is due to uncertainty of occupant behavior (i.e. leaving windows opened), multiple setpoint schedules, different operational schedules for VAV-preheat coil and radiant panels, and modeling assumptions and errors. Hourly MBE and CV (RMSE) for heating loads are 0.96% and 18.3%, respectively, while, -0.45% and 8.63% for cooling. The results are within the ASHRAE Guideline 14-2002 thresholds. After the model was calibrated against measured data, Sankey diagrams on the building-level were developed using historical data and data from BPS model.

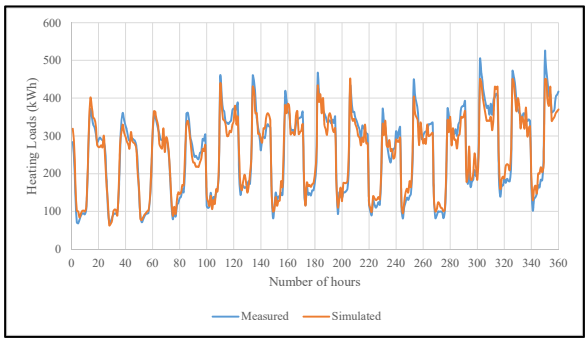

Figure 6: Hourly heating loads

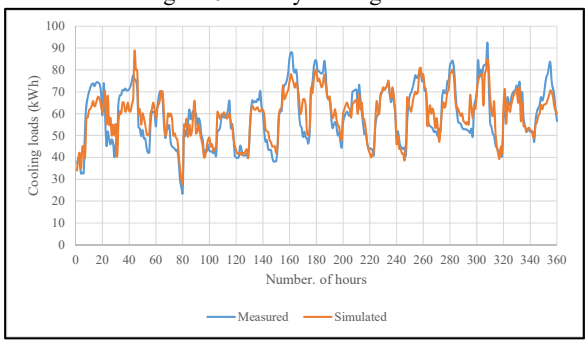

Figure 7: Hourly cooling loads

Sankey diagrams should be read based on the direction of the flow (i.e. from left to right). All energy inputs come from the left side, while energy outputs leaves rightward. For instance, during winter, heat is added to the building. While during summer, heat is extracted from the building.

The heating demands recorded high values compared to a new commercial buildings energy use intensity in Canada (~500 kWh/m^2) (NRCan, 2013 a). This is partially due to the fact that the set point temperature is set to 22°C and ventilated all the day, which is not related to occupancy presence (i.e. based on arrival and departure time). Moreover, some spaces had their windows permanently left open in the winter. And importantly, opposite pairs of large sliding doors at the entrance causes significant airflow through the building lobby. Approximately 60 percent of heat added is from the steam delivered from the CHP during winter days. The steam delivered passes through a heat exchanger that uses the thermal energy to provide heat to AHU-heating coils, VAV-preheat coils, and radiant panels in some rooms. While, 40 percent of heat is added from internal gains (i.e. equipment, lighting, and high occupancy levels) and heat gain from windows as shown in Figure 8.

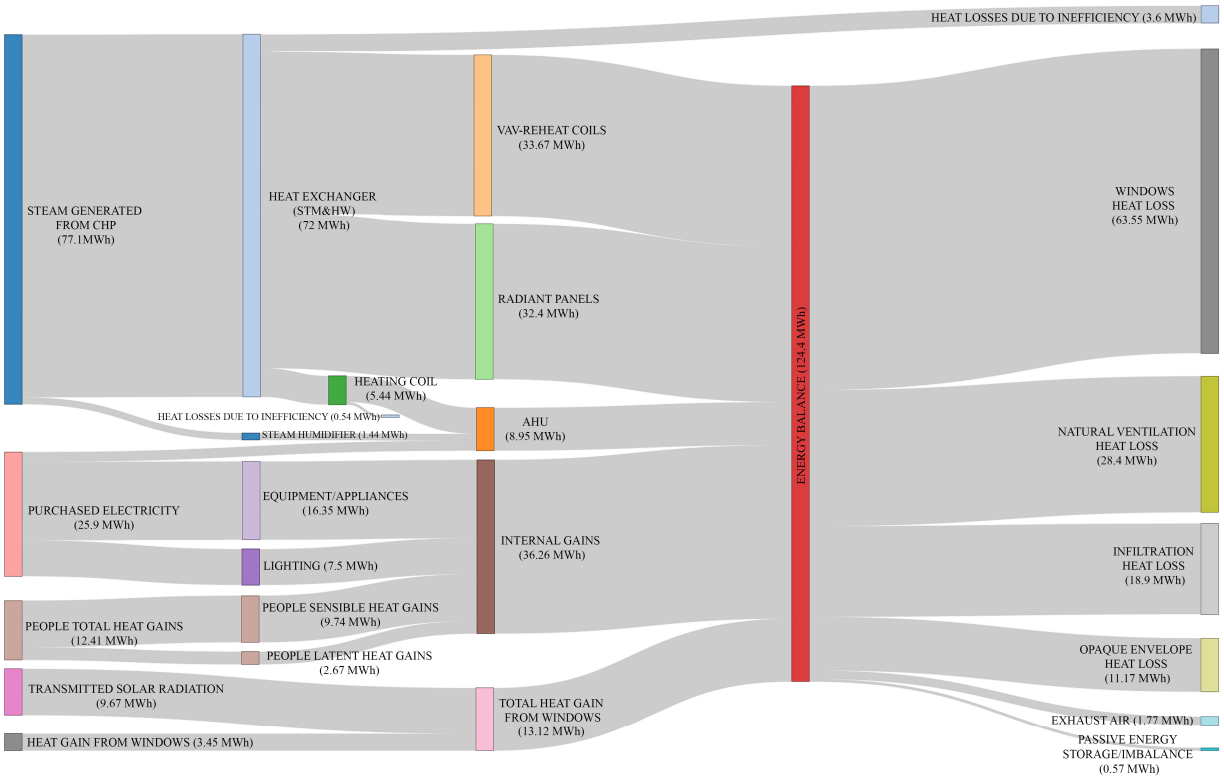

Figure 8: Sankey diagram showing building-level energy flow during two winter weeks

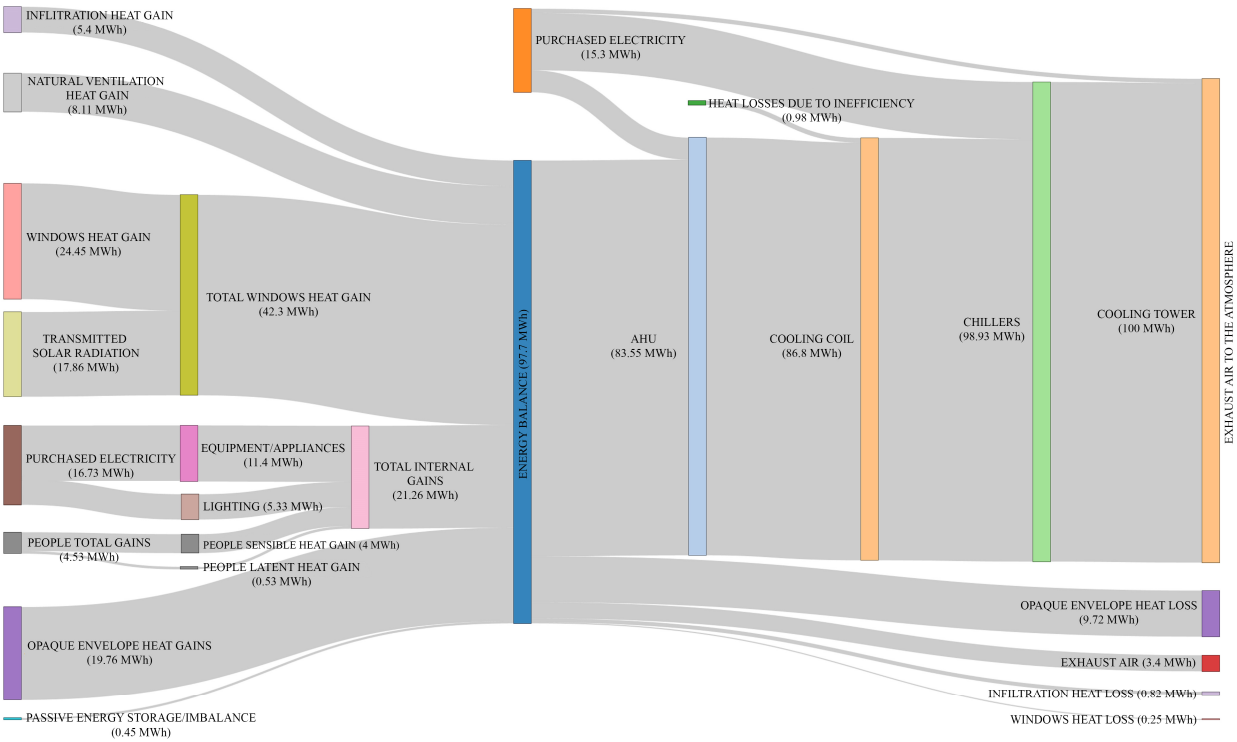

Figure 9: Sankey diagram showing building-level energy flow during two summer weeks

The sources of heat gain from windows are from direct transmitted solar radiation and the amount of solar radiation that is absorbed by the window that transfer heat by radiation or convection. Furthermore, the highest source of heat loss in the winter period is from windows due to the high temperature difference between outdoor (ranges from -26 to -5°C) and indoor (ranges from 20 to 22°C) and relatively high U-value. On the other hand, during summer days, around 85 percent of the heat extracted is from the AHU-cooling coils as shown in Figure 9. The refrigerant (water-propylene glycol) for the case study building) extracts heat from the water in the cooling coils and transfers it to the condensing water by chillers. The cooling tower extracts heat from the condensing water. Moreover, some of the heat is exhausted to the environment from AHU-exhaust dampers.

Moreover, it was noticed that the lighting consumption is high during unoccupied hours for security purposes; they were left on for hallways, lobby, and washrooms. While, some of the teaching labs and some occupants leave their PCs switched-on during unoccupied hours, which leads to a high energy consumption for plug loads.

On the hand, some of the teaching labs and some occupants leave their computers switched-on during unoccupied hours, which leads to a high-energy consumption for plug loads.

CONCLUSION

The aim of the study was to visualize and analyze energy flow on the building level. The methodology was applied to a multi-zone Canadian university building. The objective of this study is to make use of real-time and historical data obtained from EMCS and model data to provide a comprehensive energy-use assessment tool that could facilitate the decision making by building operators.

The implication of this work is that it will help make operational problems more visible and quantifiable in order to identify opportunities for energy savings. Moreover, it will also help in quantifying unmeasured energy flows through a hybrid measurement-simulation approach.

ACKNOWLEGEMENTS

The generous support of Autodesk and the Natural Sciences and Engineering Research Council are acknowledged. Furthermore, this research would not be possible without the tireless ongoing support of Carleton University's Facilities Management and Planning, Delta Controls, and Regulvar.

REFERENCES

Abdelalim, A., O'Brien, W. and Shi, Z. (2015), "Visualization of Energy and Water Consumption and GHG Emissions: A Case Study of a Canadian University Campus," Energy and Buildings, vol. doi:10.1016/j.enbuild.2015.09.058.

Beausoleil-Morrison, I. (2002), "The Adaptive Simulation of Convective Heat Transfer at Internal Building Surfaces," Building and Environment, vol. 37, no. 8-9, pp. 791-806.

Belzer, D. (2006), "Energy End-Use Flow Maps for the Buildings Sector," Pacific Northwest national Laboratory, Springfield, VA.

Coakley, D., Raftery, P. and Molloy, P. (2012), "Calibration of Whole Building Energy Simulation Models: Detailed Case Study of a Naturally Ventilated Building Using Hourly Measured Data," in First Building Simulation and Optimization Conference, no. September, 57-64.

Dong, B., Zheng, O. and Li, Z. (2014), "A BIM-enabled Information Infrastructure for Building Energy Fault Detection and Diagnostics," Automation in Construction, vol. 44, pp. 197-211.

Gowri, K., Winiarski, D. and Jarnagin, R. (2009), "Infiltration Modeling Guidelines for Commercial Building Energy Analysis," Pacific Northwest National Laboratory, Oak Ridge, TN.

Heidt, F. (2012), "CASAnova". http://nesa1.unisiegen.de/index.htm?/softlab/casanova_e.htm. As of 20 February 2015.

Heo, Y. (2011), "Bayesian Calibration of Building Energy Models for Energy Retrofit Decision-Making under Uncertainty," PhD Thesis, Georgia Institute of Technology, Georgia.

Lam, K. P., Zhao, J., Ydstie, E. B., Wirick, J., Qi, M. and Park, J. (2014), "An Energyplus Whole Building Energy Model Calibration Method For Office Buildings Using Occupant Behavior Data Mining And Empirical Data," in ASHRAE/IBPSA-USA Building Simulation Conference, Atlanta, GA.

LBNL (2011), "GenOpt," Lawrence Berkeley National Laboratory, Berkeley, CA.

Liddament, M. (1986), "Air Infiltration Calculation Techniques—an Applications Guide," Bracknell, Berkshire.

Lucid (2014), "Building Dashboard". http://www.luciddesigngroup.com/buildingdashboard/index.html. As of 24 February 2015.

M. Santamouris (2010), Energy Performance of Residential Buildings: A Practical Guide for Energy Rating and Efficiency, Taylor & Francis.

MacDonald, I. (2002), "Quantifying the Effects of Uncertainty in Building Simulation," Ph.D. Thesis University of Strathclyde, United Kingdom, Strathclyde, United Kingdom.

McGill University (2015), "McGill Energy Dashboard". https://my.pulseenergy.com/mcgill/dashboard#/location/1585. As of 26 February 2015.

Ng, L. C., Persily, A. K. and Emmerich, S. J. (2015), "Improving Infiltration Modeling in Commercial Building Energy Models," Energy and Buildings, vol. 88, no. 1, p. 316–323.

NRCan (2013), "Survey of Commercial and Institutional Energy Use: Establishments 2009," Natural Resources Canada, Ottawa.

NRCan (2014), "HVAC & Energy Systems," Natural Resources Canada. http://www.nrcan.gc.ca/energy/efficiency/housing/research/3937. As of 2 November 2015.

O'Brien, W. (2012), "Preliminary Investigation of The Use of Sankey Diagrams to Enhance Building Performance Simulation-Supported Design," in Symposium on Simulation for Architecture and Urban Design. Society for Computer Simulation International.

Perez, R., Ineichen, P., Seals, R., Michalsky, J. and Stewart, R. (1990), "Modeling Daylight Availability and Irradiance Components from Direct and Global Irradiance," Solar Energy, vol. 44, no. 5, pp. 271-289.

Phineas (2015), "Visualizing Internal and External Heat Flow," Sankey Diagrams. http://www.sankey-diagrams.com/visualizing-internal-and-external-heat-flow/. As of 10 December 2015.

Raftery, P., Keane, M. and Costa, A. (2011), "Calibrating Whole Building Energy Models: Detailed Case Study Using Hourly Measured Data," Energy and Buildings, vol. 43, no. 12, pp. 3666-3679.

Sefaira (2012), "Sefaira". http://sefaira.com/ our-resources/. As of 18 February 2015.

Silva, A. S. and Ghisi, E. (2014), "Uncertainty Analysis of User Behaviour and Physical Parameters in Residential Building Performance Simulation," Energy and Buildings, vol. 76, pp. 381-391.

Simeb (2011), "ExCalibBEM" Simeb. https://www.simeb.ca/ExCalibBEM/index_fr.php. As of 3 October 2015.

Sun, J. and Reddy, T. A. (2006), "Calibration of Building Energy Simulation Programs Using the Analytic Optimization Approach (RP-1051)," HVAC&R Research, vol. 12, no. 1, pp. 177-196.

Thevenard, D. and Haddad, K. (2006), "Ground Reflectivity in the Context of Building Energy Simulation," Energy and Buildings, vol. 38, pp. 972-980.

UBC (2014a), "UBC Energy Demand". https://my.pulseenergy.com/ubc/dashboard#/overview. As of 26 Febrarury 2015.

US-DOE (2009), "EnergyPlus Energy Simulation Software" U.S. Department of Energy. http://apps1.eere.energy.gov/buildings/energyplus/. As of 9 September 2015.

U.S. Department of Energy (2014), "Weather Data Sources" U.S. Department of Energy: Energy Efficiency and Renewable Energy. http://apps1.eere.energy.gov/buildings/energyplus/weatherdata_sources.cfm#TMY2. As of 26 October 2015.

Yarbrough, I., Reeves, Q. S. D., Hackman, K., Bennett, R. and Henshel, D. (2014), "Visualizing Building Energy Demand for Building Peak Energy Analysis," Energy and Buildings, vol. 91, no. 1, p. 10–15.